propylene or 1-butene. There appears to be only a slight increase at most in the concentration of the C+1 product when olefin of carbon number C is added. This is consistent with the above studies, namely that any chain incorporation effect is small or negligible.

The slope of the line yields the value of $\alpha = 0.43$ for the C_3-C_7 fraction. This is much lower than the 0.55-0.65 range we normally observe on this catalyst with feed gas H_2/CO ratios from 0.5 to 1.8. This appears to be caused by the high (H_2/CO) ratios present. Figure 9 shows Flory plots for data obtained at H_2/CO feed ratios of approximately 10 and 50 at each of three total pressures. There is no effect of pressure as such, but the higher H_2/CO ratio feed results in a lower α and a greater relative ethane production.

1D. Synthesis Gas Composition

A systematic study was made here of the effects of temperature and feed ratio on the prereduced fused magnetite catalyst.

Light Products

Figure 10 is a plot of α_1 as determined from the C_3-C_7 products versus CO/H_2 ratio existing in the reactor. The data are from runs with H_2/CO feed ratios from 0.5 to 1.8 (232-263°C; 0.45-1.48 MPa) obtained earlier in our laboratory, to which we have added a set of runs obtained in the present study with H_2/CO feed ratios of 5-50, at 232°C and 0.30-0.79 Pa. Values of α_1 appear to be relatively independent of CO/H_2 ratio, except at

very low reactor CO/H_2 ratios.

This relationship is almost linear on a semilog plot, as shown in Figure 11. Dictor and Bell (1986a) have also reported values of α_1 on the C-73 fused iron catalyst using the C_1-C_7 fraction, from data obtained at 231-285°C and total pressures of 0.3-1.3 MPa. Their data fall on our correlation, as shown in Figure 12.

The effects of reactor CO/H_2 ratio on α_1 for five different iron catalysts are compared in Figure 13. The Schliebs and Gaube data (1985) were obtained on precipitated iron catalysts, promoted with K or unpromoted, at 260°C and 1.0-1.2 MPa. Their data have the same general trend with CO/H_2 ratio as our data, but the range of CO/H_2 ratios they studied is narrower. The values of α_1 of Schliebs and Gaube, in general, are about 10% lower than our data at the same CO/H_2 ratio. Their values of were calculated by fitting a two-α model to their data, in contrast to our method here that used the C_3-C_7 range to calculate α_1. If this difference were taken into account, we would obtain very similar values for α_1 for our fused iron catalyst and their promoted and unpromoted precipitated catalysts.

Dictor and Bell (1986a) seem to have included data from the transition region, which would increase the influence of α_2 on their calculated α_1 values. This would be particularly true for the potassium-promoted catalyst since potassium appears to increase the contribution of products from α_2. If this factor

were taken into account, the difference between our data, the data of Schliebs and Gaube, and the data of Dictor and Bell, would be quite small. This would suggest that the value of α_1 is relatively insensitive to the form or method of preparation of the iron catalysts, or to the presence or absence of potassium within the ranges studied.

We find no effect of temperature on α_1 from the fused magnetite catalyst, as shown in Figure 14. This brings together our present studies at 310°C, and present studies at 230°C and high H_2/CO ratios. Dictor and Bell (1986a) also did not find significant changes with temperature in the range 248-285°C on this fused iron catalyst.

1.E. Poisoning by Sulfur Compounds

In an earlier paper (Stenger and Satterfield, 1985), we reported effects of sulfur poisoning on the Fischer-Tropsch synthesis as carried out on a prereduced fused magnetite catalyst in a slurry reactor. Studies were done with H_2S or dibenzothiophene (DBT). The two poisons behaved quite differently. With H_2S, small additions increased catalyst activity up to a maximum at a sulfur loading of 1.3 mg of sulfur/g of Fe, beyond which activity decreased. This effect was not observed with DBT. H_2S poisoning had no significant effects on the C_1-C_5 product distribution whereas DBT significantly decreased the formation of C_1 and C_2 products. Both poisons decreased secondary hydrogenation of olefins to paraffins, but the effect was more marked with DBT at higher H_2 pressures.

There was an important difference between the way in which the catalyst was poisoned with the two sulfur compounds. In both cases the catalyst was prereduced to the metallic form. However H_2S was contacted with the catalyst only after it had reached steady-state activity in the presence of synthesis gas and was predominantly in the carbidic form. In contrast, in studies with DBT, the sulfur compound was contained in the suspending liquid initially and hence was present while the prereduced catalyst was being converted form the metallic form to the predominantly carbidic form.

To help clarify the above observations, we studied the effects of adding dibenzothiophene onto a prereduced versus a carburized fused magnetite catalyst. Detailed results have been published (Matsumoto and Satterfield, 1987).

We concluded that a fused magnetite catalyst is more readily poisoned with respect to activity by dibenzothiophene (DBT) if the catalyst is prereduced rather than precarburized. Apparently the DBT is much more readily adsorbed onto the prereduced catalyst. For a given sulfur loading on the catalyst, there is a greater loss in activity than if the same sulfur loading is achieved by adsorption of H_2S. Thus, at a sulfur loading of 3.3 mg of S/g of Fe, activity was reduced to about 10% of its original value, whereas when this loading was achieved from H_2S, activity reduction was only about 50%.

With the precarburized catalyst, repeated dosing with DBT caused no further increase in sulfur loading on the catalyst

above about 1 mg of S/g of Fe. This suggests that some plateau in degree of adsorption may exist for the precarburized catalyst with a corresponding activity of about 50% of original.

The kinetic data from the precarburized/poisoned catalyst experiments fit the form of the expression proposed by Huff and Satterfield (1984) and yielded about the same activation energy, suggesting that the same basic Fischer-Tropsch mechanism is occurring in both poisoned and unpoisoned systems.

2A. Wax Analyses

Gas chromatograms showed no evidence of secondary reactions of the heavy product at temperatures of 232-263°C, but considerable secondary reactions seemed to occur at 310°C, as shown in Fig. 15. This compares gas chromatograms for the wax synthesized at the two different temperatures.

An unsually high density of peaks followed the octacosane peak in the chromatograms from the bonded methylsilicone capillary column used for wax analyses. (Octacosane is the liquid initially present in the reactor before synthesis begins.) This multitude of components was not observed at 232-263°C. Treatment of a sample of wax from a 310°C run with hydrogen over a carbon-supported rhodium catalyst yielded no noticeable peak shifts, indicating that the new peaks were probably not olefinic or aromatic in nature. Since these products appeared after the octacosane peak, it is probable that these are formed by a reaction with the octacosane carrier, perhaps by some alkylation process. The same kind of reactions would presumably occur with

any paraffinic material present at this temperature.

To eliminate the influence of what appeared to be a secondary process, we assumed that the normal paraffins present would indicate the true chain growth probability for the primary products from the catalyst. A run at 310°C with H_2/CO = 3.8 feed gas, produced strong normal paraffin peaks in the chromatograms, allowing for easier identification. Figure 16 shows the results from the two runs at 310°C and one at 234-269°C on the C-73 catalyst. For clarity in presentation the three sets of data are displaced from one another by expressing concentration for each set in arbitrary units. For the lower temperature the α based on C_{33}-C_{43} (except C_{38}) is 0.89.

The data for the two high-temperature runs definitely have steeper slopes, indicating lower values of α. Deviations from a linear fit of the data occur here in the C_{28}-C_{32} and C_{36}-C_{39} regions. The former region is affected by impurities in the octacosane as well as the tail from the octacosane peak in the chromatograms. The latter region is affected by the "crossing" of product peaks through the normal paraffin peaks, that is, a series of product peaks that appear after the normal paraffins early in the chromatogram and gradually end up ahead of the normal paraffins later in the chromatogram. For carbon numbers 36-38, the peaks cannot be resolved and thus the normal paraffins appear to be in greater concentration than they actually are. Because of the higher concentration of normal paraffins in the run using $(H_2/CO)_{in}$ = 3.8, this effect was less pronounced than

in the run using $(H_2/CO)_{in}$ = 0.7. If the carbon numbers in the above regions are neglected, the α_2 values for the high-temperature runs are about 0.82.

Discussion of α_2 for Heavier Products

Knowledge of α_2 from other studies is more limited because of the difficulty in obtaining representative data. The analysis of the pot wax in the reactor, while it yields a wide range of carbon numbers over which to determine α_2, represents the total accumulated products for all conditions run previous to sampling. Table 4 shows that the range of values of α_2 we have observed from analysis of pot wax for a fused-magnetite catalyst in our previous studies in the temperature range of 2132-263°C is 0.89-0.93 (Huff and Satterfield, 1984; Stenger, et al., 1984). Values taken from a number of other reports are also given. The data from the precipitated catalysts used in the Schwarzheide tests are also in about the same range as are results from the proprietary catalyst used by Mobil.

α_2 clearly decreaes significantly with increased temperature. The common observation that increased potassium content increases the average carbon number can be interpreted as increasing the fraction of the total product formed by the mechanism leading to α_2. Further details have been published by Matsumoto and Satterfield (1989).

2B. Theoretical Analysis of Data to Determine C-number Product Distributions

Figure 17 shows a representative Flory plot for the overhead products from a stirred autoclave reactor. There are three regions; the first two are usually modeled with a Flory-type distribution using two independent chain growth parameters, α_1 and α_2. In region III accumulation of relatively less volatile products in the reactor causes the overhead distribution to drop off from the true product composition with increasing molecular weight. An analogous problem occurs in a fixed-bed reactor associated with liquid accumulation effects in catalyst pores. We have published some theoretical analyses of this effect (Huff and Satterfield, 1985) and also some brief analyses of the time required for a specified percentage of paraffin product of carbon number n to have appeared overhead from an autoclave reactor (Huff and Satterfield, 1984).

The transition from region I to region II can be quite broad, making determination of the underlying chain growth parameters difficult. This can be made worse by a narrow region II, limiting the number of representative points. We have developed a general method for calculating the correct values of α_1 and α_2 from data that include contributions by both chain growth probabilities. The causes of two probabilities for chain growth are unclear, but the method is not based on any assumptions about the cause of the double-α.

The most straightforward method for determining α_1 and α_2

from experimental data would seem to be linear regression of the asymptotes of a Schulz-Flory plot. Figure 18 shows a typical Schulz-Flory diagram from a potassium-promoted precipitated iron catalyst. The diagram shows regions with two distinct slopes. However, even several carbon numbers away from the intersection of the two lines, the values of α_1 and α_2 determined by linear regression differ by 5-10% from those calculated by a rigorous statistical procedure that we have developed. Simple linear regression over small carbon number ranges can only approximate α_1 and α_2.

In calculating α_1 and α_2, our method uses the entire experimental product distribution including those points between the asymptotes. Excellent agreement between the regression and experimental data from iron catalysts has been shown. For an unalkalized precipitated iron catalyst, experimental data from an overhead product stream are fit by the regression and the value of α_2 is shown to agree with that calculated from a slurry wax sample. In addition, product stream data from a fused magnetite catalyst are fit.

Details of the model and its use are published elsewhere (Donnelly, et al., 1988). Basically it is a nonlinear regression method that calculates the three parameters needed to characterize the C-number distribution, α_1, α_2 and ξ (the break point).

2C. Observed Product Distribution during Start-Up (Fused Magnetite)

In studies at 232 and 248°C and 0.92 MPa, during the first 20 hours on stream both Fischer-Tropsch synthesis activity and CO consumption increase to quasi-steady-state values (Fig. 19). During this time the bulk catalyst, initially α-Fe, was converted to a mixture of α-Fe and iron carbides, as determined by Mossbauer spectroscopy (Fig. 20). At 248°C, the carbide formed was χ-Fe_5C_2. At 232°C, χ-Fe_5C_2 and, to a lesser extent, ξ'-$Fe_{2.2}C$ formed. At neither temperature was magnetite formed. During the first few hours, methane selectivity decreased markedly while the olefin/paraffin ratio increased (Figures 21 and 22). Subsequently, methane selectivity increased, the olefin/paraffin ratio decreased, and the β-olefin/α-olefin ratio increased (Fig. 23), but all these effects occurred quite slowly. No change was observed in the C_2-C_8 product distribution with time on stream.

The water-gas-shift selectivity attained steady state within the first several hours at 248°C and within about 15 hours at 232°C. For further details see Satterfield et al. (1986a).

2D. Effect of Water

At high conversions the product gases may contain various amounts of water, depending upon the activity of the catalyst for the water-gas shift reaction. We found that the deliberate addition of water vapor to dry synthesis gas to comprise as much as 27 mol % of the feed composition decreased catalyst activity,

but the effect was completely reversible upon removal of the water vapor (Fig. 24). A1, A2, A3 and A4 correspond to original conditions without water addition. Reversibility was not complete with water addition to comprise 42 mol % of feed. Water vapor decreased methane selectivity (Fig. 25), increased oxygenate selectivity (Fig. 26), and increased the rate of the water gas shift. However, these effects did not correlate with the relative Fe_5C_2, Fe_3O_4, and Fe content of the bulk catalyst as determined by Mossbauer spectroscopy, although the Fe_5C_2 content did not change greatly. Molecular weight distribution of the C_3-C_7 products was not affected by water (Fig. 28). For further details see Satterfield et al. (1986b).

3A. Performance Testing

A mechanically-stirred, slurry reactor for study of the Fischer-Tropsch synthesis offers excellent temperature control and flexibility in operating conditions. Since the internal composition of such reactors is uniform, they facilitate development of kinetic models without the complications involved in analysis of integral data obtained in a fixed-bed reactor.

Regardless of the type of reactor, it is necessary to design flow, temperature, and pressure control systems that allow steady-state operation. It is also necessary to collect and analyze a wide range of condensable and non-condensble products to analyze hydrocarbon and oxygenate distributions. Gas chromatography offers considerable flexibility in analyzing hydrocarbon and oxygenated products over a wide range of

molecular weights, but care must be taken in developing analytical algorithms. Care must also be taken to avoid mass transfer limitations. In slurry reactors, low-density catalysts may be entrained by exit vapors, and finely divided catalyst particles may also be difficult to separate from slurry waxes. Some apparent discrepancies in the literature regarding catalyst activity and selectivity in Fischer-Tropsch synthesis can be explained by analysis of the pertinent experimental systems.

Useful methods are discussed in detail in Appendix B.

3B. Effect of CO_2 on Fischer-Tropsch Kinetics

Except for one early publication, all the kinetic expressions that have been published until recently for the rate of synthesis assume that there is no inhibiting effect of CO_2 on the rate. The rate expression of Anderson (1956, p. 227), frequently referenced, is

$$-R_{H_2+CO} = aP_{H_2}P_{CO}/P_{CO} = bP_{h_2O} \qquad (3)$$

Anderson noted that for a fixed temperature the two constants showed a definite, but undisclosed, trend with feed gas composition.

Huff and Satterfield (1984), using a well-mixed continuous flow slurry reactor, more recently developed an improved rate expression:

$$-R_{H_2+CO} = ab'P_{CO}P_{H_2}{}^2/P_{H_2O} = b'P_{CO}P_{H_2} \qquad (4)$$

In most previous kinetic studies, the partial pressure of hydrogen did not vary significantly with conversion because the

consumption of hydrogen was nearly offest by the contraction that accompanies reaction. Consequently, the dependence of the rate on hydrogen pressure was not clearly established. In eq. 4, b' is a function of temperature only, but eq. 4 reduces to the form of eq. 3 if b in eq. 3 is inversely proportional to P_{H_2}. Both eq. 3 and 4 neglect possible inhibition by Co_2 and include that by H_2O only. Both equations reduce to the same form at low H_2O partial pressures. In our development of eq. 4, the concentration of CO_2 did not seem to be an important variable, but conditions in which a high ratio of CO_2 to H_2O existed were not studied systematically.

Recently, Deckwer and co-workers have published three papers presenting kinetic studies performed in a slurry reactor using either a magnetite catalyst or a precipitated iron catalyst promoted with potassium. At H_2/CO inlet ratios of 0.8 and less, they concluded that water concentration was negligible based on stoichiometric calculations, but this assumption was not tested experimentally. They correlated their data by the expression

$$-R_{H_2+CO} = b_1 C_{H_2}/1 + b_2 C_{CO_2}/C_{CO} \qquad (5)$$

In view of the recommended correlation of eq. 5, we examined possible inhibition effects of CO_2 by deliberately adding it to synthesis gas and analyzing for the actual water concentration present.

We conclude that the inhibition attributed to CO_2 in eq. 5 was instead caused by water formed from CO_2 by the reverse water gas shift reaction. Inhibition effects by H_2O swamp those

possibly caused by CO_2.

Further details have been published (Yates and Satterfield, 1989).

References

R.B. Anderson, in P.H. Emmett, (Ed.), Catalysis, Vol. 4, Rheinhold, New York, 1956, p. 119.

D.B. Bukur and R.F. Brown, Can. J. Chem. Eng., 65 (1987) 604.

L. Caldwell, Selectivity in the Fischer-Tropsch Synthesis, CSIR Report CENG 330, Pretoria, 1980.

R.A. Dictor and A.T. Bell, Appl. Catal. 20 (1986a) 145.

R.A. Dictor and A.T. Bell, J. Catal., 97 (1986b) 121.

T.J. Donnelly, I.C. Yates, and C.N. Satterfield, Energy and Fuels, 2 (1988), 734.

T.J. Donnelly and C.N. Satterfield, Applied Catalysis, 52 (1989) 93.

M.E. Dry, in J.R. Anderson and M. Boudart (eds.), Catalysis Science and Technology, Vol. 1, Springer-Verlag, New York, 1981, p. 159.

R.T. Hanlon and C.N. Satterfield, Energy & Fuels, 2 (1988) 196.

G.A. Huff, Fischer-Tropsch Synthesis in a Slurry Reactor. Sc.D. Thesis, Massachusetts Institute of Technology, 1982.

G.A. Huff and C.N. Satterfield, Ind. Eng. Chem. Process Des. Dev., 23 (1984) 696.

G.A. Huff and C.N. Satterfield, Ind. Eng. Chem., Process Des. Dev., 24 (1985) 986.

H. Itoh, H. Hosaka, T. Ono and E. Kukuchi, Appl. Catal., 40 (1988) 53.

L. Konig and J. Gaube, Chem.-Ing. Tech., 55 (1983) 14.

J.C.W. Kuo, Slurry Fischer-Tropsch/Mobil Two-Stage Process of Converting Syngas to High Octane Gasoline, Final Report, DOE/PC/30022-10 (DE84004411), 1983.

J.C.W. Kuo, Two-Stage Process for Conversion of Synthesis Gas to High Quality Transportation Fuels, Final Report, DOE/PC/60019-9, 1985.

D.K. Matsumoto and C.N. Satterfield, Energy & Fuels, 1 (1987) 203.

D.K. Matsumoto and C.N. Satterfield, Energy and Fuels, 3 (1989) 249.

C.N. Satterfield et al., I&EC Product Res. and Devel., 25 (1986a) 401.

C.N. Satterfield et al., I&EC Product Res. and Devel., 25 (1986b) 407.

B. Schliebs, Untersuchungen zur Selektivitat der Fischer-Tropsch-Synthese an Eisenkatalysatoren, Dr.-Ing. dissertation, Technische Hochschule, Darmstadt, 1983.

B. Schliebs and J. Gaube, Ber. Bunsenges. Phys. Chem., 89 (1985) 68.

H.G. Stenger, H.E. Johnson and C.N. Satterfield, J. Catal., 86 (1984) 477.

H.G. Stenger and C.N. Satterfield, Ind. Eng. Chem. Process. Des. Dev., 24 (1985) 415.

I.C. Yates and C.N. Satterfield, Ind. Eng. Chem. Res., 28 (1989), 9.

M.F. Zarochak, M.A. McDonald and V.U.S. Rao, Stability and Selectivity of Potassium Promoted Iron Catalyst in Slurry Fischer-Tropsch Synthesis, 12th Annual Conference on Fuel Sciences, Palo Alto, May 13-14, 1987. Also private communication from Zarochak (1985).

List of Figures

Figure 7 Effect of 1-decene addition. A slight increase in the $C_{11}+$ fraction is observed with overlapping points at C_2 and C_{13}. Data normalized by excluding C_{10} fraction. Total pressure = 0.92 MPa.

Figure 8 Effect of added olefin on Fischer-Tropsch carbon number distribution. H_2/CO in feed = 5; total pressure = 0.79 MPa. No significant effect is observed.

Figure 9 Effect of H_2/CO feed ratio on carbon number distribution.

Figure 10 Effect of reactor CO/H_2 ratio on α_1.

Figure 11 Log plot of abscissa of Figure 10 to separate data at low CO/H_2 ratios.

Figure 12 Comparison of present data and that of Huff with data of Dictor and Bell, all obtained on fused-magnetite catalyst C73.

Figure 13 Comparison of α_1 versus CO/H_2 ratio from several iron catalysts.

Figure 14 Comparison of α_1 for high- and low-temperature runs.

Figure 15 Gas chromatograms from high- and low-temperature runs.

Figure 16 Heavy product analyses from high- and low-temperature runs.

Figure 17 General form of the Schulz-Flory plot for reactor effluent from an iron catalyst.

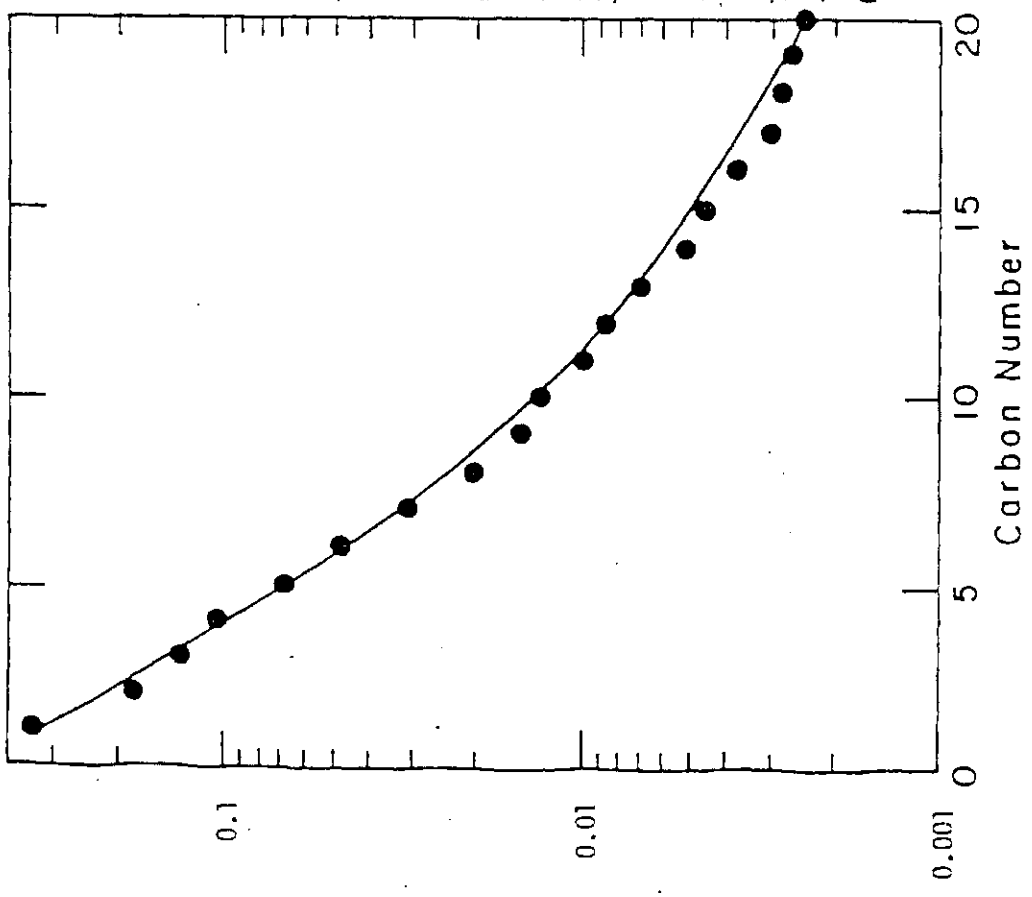

Figure 1. Schulz-Flory diagram of volatile products from an unalkalized precipitated iron catalyst. 260°C, 1.48 MPa, 0.02 Nl/min/g_{cat}, $(H_2/CO)_{feed}$ = 1.0, 665 hours-on-stream.

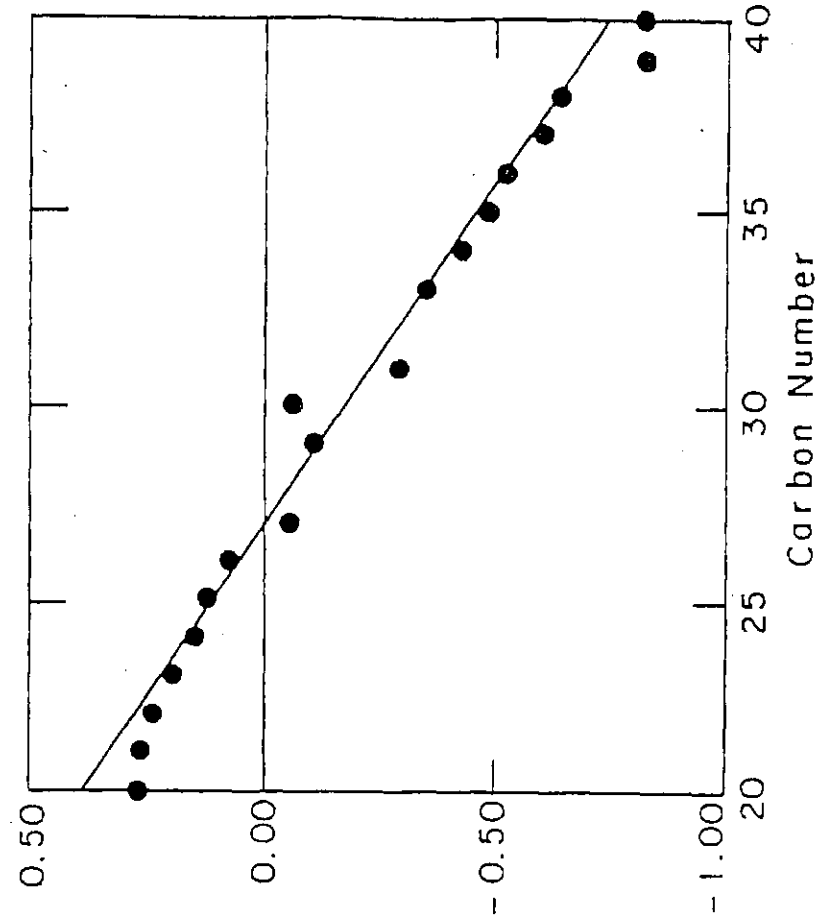

Figure 2. Schulz-Flory diagram of reactor wax from an unalkalized precipitated iron catalyst. 260°C, 1.48 MPa, 0.02 Nl/min/g_{cat}, $(H_2/CO)_{feed}$ = 1.0, 170 hours-on-stream.